CrossMark

Dye-decolorizing peroxidases in *Irpex lacteus* combining the catalytic properties of heme peroxidases and laccase play important roles in ligninolytic system

Xing Qin[1,2], Huiying Luo[2], Xiaoyu Zhang[1], Bin Yao[2], Fuying Ma[1*] and Xiaoyun Su[2*]

Abstract

Background: The white rot fungus *Irpex lacteus* exhibits a great potential in biopretreatment of lignocellulose as well as in biodegradation of xenobiotic compounds by extracellular ligninolytic enzymes. Among these enzymes, the possible involvement of dye-decolorizing peroxidase (DyP) in lignin degradation is not clear yet.

Results: Based on the extracellular enzyme activities and secretome analysis, *I. lacteus* CD2 produced DyPs as the main ligninolytic enzymes when grown in Kirk's medium supplemented with lignin. Further transcriptome analysis revealed that induced transcription of genes encoding DyPs was accompanied by the increased expression of transcripts for H_2O_2-generating enzymes such as alcohol oxidase, pyranose 2-oxidase, and glyoxal oxidases. Meanwhile, accumulation of transcripts for glycoside hydrolase and protease was observed, in agreement with abundant proteins. Moreover, the biochemical analysis of *Il*DyP2 and *Il*DyP1 confirmed that DyPs were able to catalyze the oxidation of typical peroxidases substrates ABTS, phenolic lignin compounds DMP, and guaiacol as well as non-phenolic lignin compound, veratryl alcohol. More importantly, *Il*DyP1 enhanced catalytic activity for veratryl alcohol oxidation in the presence of mediator 1-hydroxybenzotriazole, which was similar to the laccase/1-hydroxybenzotriazole system.

Conclusions: The results proved for the first time that DyPs depolymerized lignin individually, combining catalytic features of different peroxidases on the functional level. Therefore, DyPs may be considered an important part of ligninolytic system in wood-decaying fungi.

Keywords: Dye-decolorizing peroxidase, White rot fungi, *Irpex lacteus*, Lignin biodegradation, Mediator

Background

Lignin is the second most abundant constituent of lignocellulosic biomass, amounting to 15–30% by weight or up to 40% by energy [1]. The degradation of lignin represents a key step for carbon recycling in the land ecosystems, as well as a critical issue for cost-effective lignocellulosic biofuels and bio-based chemicals [2]. However, due to the complex and random phenylpropanoic polymeric structure, lignin is highly recalcitrant toward chemical and biological degradations [3], resulting in lignocellulosic waste and environment pollution. White rot fungi, a large group of wood-decaying basidiomycetes, are able to completely decompose lignin into carbon dioxide and water by extracellular ligninolytic enzymes, which include an array of heme peroxidases and oxidases [4]. Among them, the heme peroxidases, such as manganese peroxidase (MnP), versatile peroxidase (VP), lignin peroxidase (LiP), and laccase (Lac) have been considered to play important roles in lignin degradation [5–7].

Dye-decolorizing peroxidase (DyP) is a member of the novel heme peroxidase family (DyP-type peroxidase superfamily), showing no homology to classic fungal

*Correspondence: mafuying@hust.edu.cn; suxiaoyun@caas.cn
[1] Department of Biotechnology, College of Life Science and Technology, Huazhong University of Science and Technology, Wuhan 430074, China
[2] Key Laboratory for Feed Biotechnology of the Ministry of Agriculture, Feed Research Institute, Chinese Academy of Agricultural Sciences, No. 12 South Zhongguancun Street, Beijing 100081, China

Qin *et al. Biotechnol Biofuels*   (2018) 11:302

Page 2 of 11

heme peroxidases including MnP, VP, and LiP [8, 9]. So far only eleven fungal DyPs have been purified and characterized [10]. Compared with classic fungal heme peroxidases, the specific feature of all DyP is the ability to oxidize synthetic high redox potential dyes of the anthraquinone type [8]. DyP can oxidize phenolic compounds, such as 2,6-dimethoxyphenol and guaiacol [7]. Recently, there are a few reports about its catalytic ability to non-phenolic lignin model compound veratryl alcohol (VA) and Mn^{2+}, which is attributed to high redox potential peroxidase LiP/VP and MnP, respectively [7, 10, 11]. These findings indicate that DyP might be an important part of ligninolytic system in white rot fungi, although biological roles of DyP are ambiguous in terms of different substrate specificities.
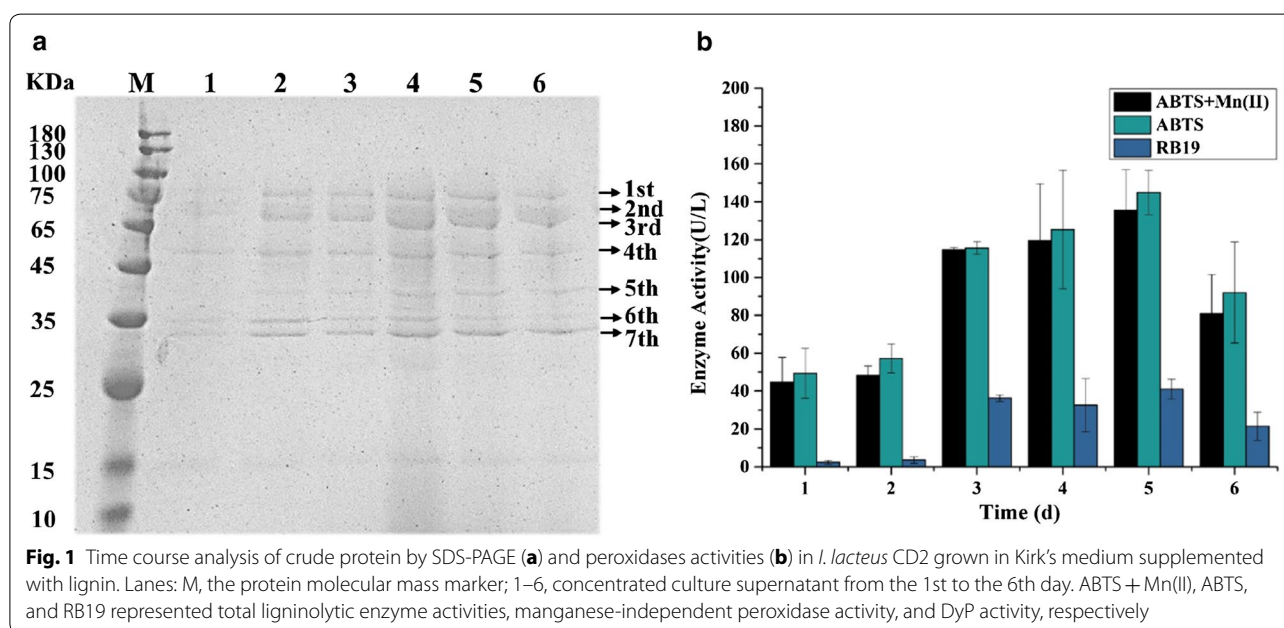
Irpex lacteus is a white rot fungus with a significant potential for various biotechnological applications such as bioremediation of organopollutants in water and soil environments and biopretreatment of lignocellulose [12, 13]. Its biotechnological applications were attributed to the extracellular ligninolytic enzymes, including MnP, LiP, laccase-like, and DyP [14–18]. Our preliminary work demonstrated *I. lacteus* CD2 could degrade all kinds of lignocellulose and dyes [13–15]. Genome analysis reveals that *I. lacteus* CD2 has seven *mnp* genes, two *lip* genes, and four *dyp* genes, without *lac* gene [14]. Compared with MnP, the main ligninolytic enzyme of *I. lacteus*, DyP is scarcely known for catalytic properties and substrate specificities, especially in lignin degradation. Herein, the main ligninolytic enzymes of *I. lacteus* CD2 grown in lignin medium were determined, combining extracellular enzyme activities and secretome analysis. Furthermore, the mechanisms of lignin degradation by the main ligninolytic enzymes DyPs were elucidated using transcriptomics and biochemical analysis.

Results and discussion

Major extracellular proteins and ligninolytic enzymes of *I. lacteus* in lignin medium

The SDS-PAGE analysis showed there were seven main bands within 30–75 kDa in extracellular proteins of *I. lacteus* in lignin medium (Fig. 1a). At the same time, extracellular ligninolytic enzyme activities were detected (Fig. 1b). There was no significant difference between total ligninolytic enzymes activity and manganese-independent peroxidases (MiPs) activity, which suggested MiPs were the main extracellular ligninolytic enzymes of *I. lacteus* CD2 in lignin medium, and MnP activity might be weak or negligible. DyPs are one of MiPs and showed the similar trend to that of MiPs in *I. lacteus* CD2 grown in lignin medium (Fig. 1a), suggesting that DyPs might be the main extracellular ligninolytic enzymes of *I. lacteus* CD2 in lignin medium. MiPs including DyP were rapidly induced since lignin and lignin-derived aromatic compounds were the most efficient inducers of ligninolytic enzymes [19]. In this study, MiPs activities increased rapidly on day 3 and obtained peaks on day 5, with maximal activities of 144.9 U/L and 41.1 U/L against ABTS and RB19, respectively (Fig. 1a). The change of protein contents was consistent with extracellular ligninolytic enzymes activities over time.

Fig. 1 Time course analysis of crude protein by SDS-PAGE (**a**) and peroxidases activities (**b**) in *I. lacteus* CD2 grown in Kirk's medium supplemented with lignin. Lanes: M, the protein molecular mass marker; 1–6, concentrated culture supernatant from the 1st to the 6th day. ABTS + Mn(II), ABTS, and RB19 represented total ligninolytic enzyme activities, manganese-independent peroxidase activity, and DyP activity, respectively

In order to determine the corresponding MiPs produced in lignin degradation, the seven gel bands on day 3 in SDS-PAGE were recovered and subjected to nano LC/MS−MS analysis. The results confirmed that DyPs were the main extracellular ligninolytic enzymes of *I. lacteus* in lignin medium (Table 1, Additional file 1). In parallel, *I. lacteus* secreted different oxidoreductases including aryl alcohol oxidase (AAO), copper radical oxidase, and cellobiose dehydrogenase (CDH) (Table 1), which can generate H_2O_2 required for the action of extracellular peroxidases [20].

In addition to ligninolytic enzymes, some proteins involving in fungal growth, such as glycosidase hydrolases (including chitinases, glucanases, mannosidases and so on) and proteases were identified in the extracellular proteins. Chitinases, glucanases, and mannosidases are involved in hyphal cell wall biosynthesis [21]. Proteases such as polyporopepsin, aspartic protease, and glutaminase are implicated in protein degradation and supplying nitrogen for fungal growth [22, 23]. Glycoside hydrolases are essential for cell wall synthesis and cell wall integrity, involving in protein maturation and transport, such as N-linked glycoproteins processing or carbohydrate structural degradation [24].

Comparative transcriptome analysis of *I. lacteus* grown in lignin and glucose medium

A total of 10,167 genes were determined from the transcriptomes of four samples: LIG3d (3 days in lignin), GLU3d (3 days in glucose), LIG6d (6 days in lignin) and GLU6d (6 days in glucose). To identify key genes and pathways associated with lignin degradation, four pairwise 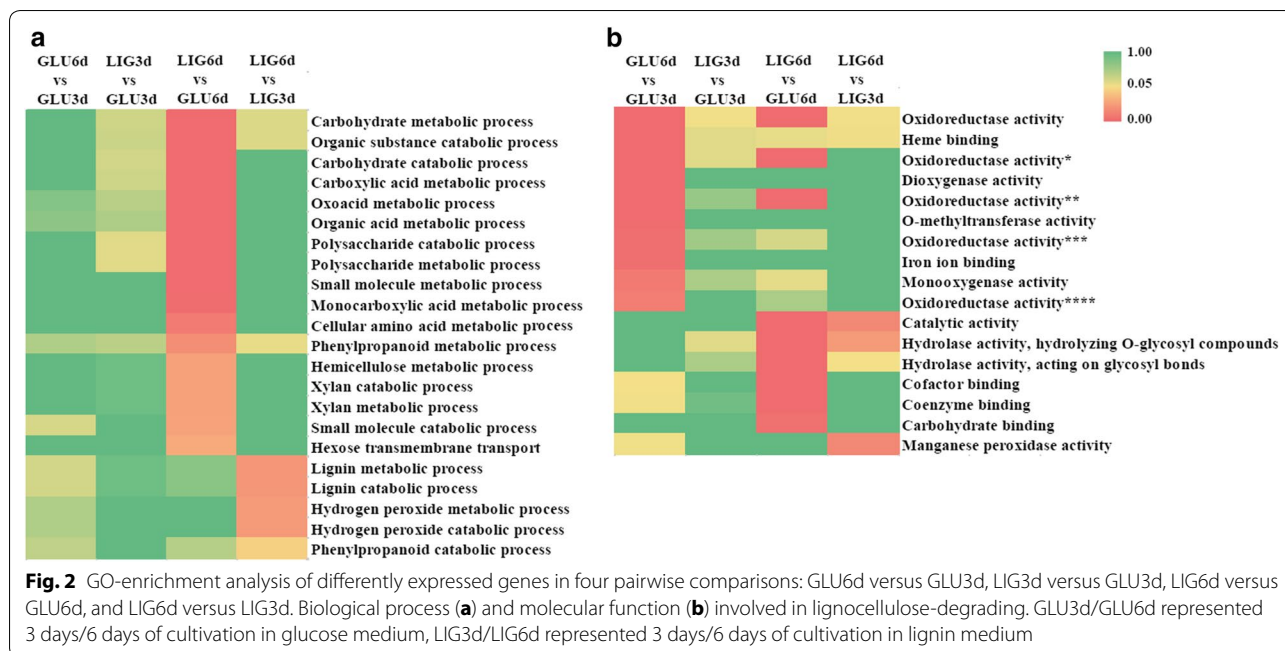comparisons were performed, including LIG3d versus GLU3d, LIG6d versus GLU6d, LIG6d versus LIG3d , GLU6d versus GLU3d. The results indicated that 4603 and 3816 genes showed at least twofold differences in comparisons of groups LIG3d versus GLU3d, and LIG6d versus GLU6d, respectively, whereas only 300 genes exhibited not less than twofold differences in the comparison of group LIG6d versus LIG3d. Moreover, GO-enrichment analysis between LIG6d versus GLU6d and LIG6d versus LIG3d revealed that these differential expression genes were significantly enriched in lignocellulose-degrading process, including lignin, carbohydrate, polysaccharide, hemicellulose, hydrogen peroxide, and phenylpropanoid metabolic/catabolic process (Fig. 2a). Besides, genes encoding oxidoreductase, heme binding, peroxidase, monooxygenase, and glycoside hydrolase (GH) were also significantly enriched (Fig. 2b). These results were in agreement with that of protein analysis. Since white rot fungi were able to produce different heme peroxidases in synergy with oxidases, and each one might contribute in different ways to the final degradation of lignin [25]. The synergetic effects of different enzymes play vital roles in depolymerizing lignin by *I. lacteus* CD2.

Ligninolytic enzyme system

Various lignin-degrading peroxidases were significantly differentially expressed along with H_2O_2-generation enzymes in *I. lacteus* in lignin medium (Fig. 3). The transcripts encoding DyPs were highly expressed in LIG3d and LIG6d, which were in agreement with extracellular peroxidases activities and protein profiles. Compared with in GLU3d, *Il*DyP1 and *Il*DyP2 in LIG3d were induced by 22.7- and 77.3-fold, then decreased by 1.5- and 3.6-fold in LIG6d, respectively. *Il*DyP4 gene was

Table 1 Major extracellular proteins identified from the SDS-PAGE bands of culture supernatant of *I. lacteus* CD2 in lignin-Kirk's medium

Number	Accession	− 10lgP	Coverage (%)	Peptides	Unique	PTM	Avg. Mass	Description
1st	0809.852	377.71	57	34	34	Y	80,666	Glutaminase
	0810.199	278.1	28	15	15	N	81,041	Glucan 1,3-beta-glucosidase
2nd	0806.17	329.07	27	13	13	Y	63,771	Aryl-alcohol oxidase
	0821.105	243.71	20	6	5	N	52,706	Dye-decolorizing peroxidase
3rd	0821.105	388.5	28	10	8	N	52,706	Dye-decolorizing peroxidase
	0807.1163	240.17	18	7	7	Y	47,202	Alpha-galactosidase
4th	0811.256	326.61	32	10	10	Y	51,332	Alpha-amylase
	0816.66	315.51	34	14	13	Y	51,687	Oxalate decarboxylase
5th	1079.46	363.17	18	6	5	N	42,231	Endo-1,6-alpha-mannosidase
	0807.283	265.31	12	7	6	N	42,718	Polyporopepsin
6th	0816.57	277.37	27	9	9	N	39,674	Endopolygalacturonase
	0807.283	271.85	12	7	6	N	42,718	Polyporopepsin
7th	0807.283	580.05	53	17	16	N	42,718	Polyporopepsin
	0925.239	446.02	36	11	10	N	43,170	Polyporopepsin

Qin *et al. Biotechnol Biofuels*   (2018) 11:302

Page 4 of 11

Fig. 2 GO-enrichment analysis of differently expressed genes in four pairwise comparisons: GLU6d versus GLU3d, LIG3d versus GLU3d, LIG6d versus GLU6d, and LIG6d versus LIG3d. Biological process (**a**) and molecular function (**b**) involved in lignocellulose-degrading. GLU3d/GLU6d represented 3 days/6 days of cultivation in glucose medium, LIG3d/LIG6d represented 3 days/6 days of cultivation in lignin medium

upregulated by 9.5-fold and further increased by 1.7-fold in LIG6d. Also, one LiP and four MnP transcripts were abundant in LIG3d, especially for *Il*MnP2. Notably, although the respective activities were not detected in the extracellular culture filtrates, MnP and LiP isoenzymes were still expressed to different extents in different stages. The similar cases were also reported in *Pleurotus ostreatus* that MnP and Lac with high transcription levels were not found in extracellular proteins, which might be inefficient secretion and the action of specific proteases [26, 27]. In addition, transcripts for one alcohol oxidases (AOX) gene, one pyranose-2-oxidase (POX) gene, and two glyoxal oxidase (GLOX) genes were significantly accumulated in LIG3d. AOX gene was upregulated by 2405.1-fold in LIG3d and decreased by 1.4-fold in LIG6d. The membrane-anchored AOX, proposed to be an extracellular source of H_2O_2 during lignin degradation [20, 28], was the most abundant transcript in H_2O_2-generation enzymes. POX gene transcript also accumulated in LIG3d and LIG6d. POX was not found in extracellular proteins in some studies, which was attributed to its location in the periplasmic space and associated with membranous materials [29, 30]. Besides, *Il*GLOX1 and *Il*GLOX2 were also induced by 135.9- and 14.8-fold in LIG3d, respectively. These suggested that AOX, POX and GLOX were implicated in providing H_2O_2 required for DyP activity.

Carbohydrate metabolism, nitrogen metabolism and related enzymes

In addition to oxidoreductases, genes encoding carbohydrate active enzymes (CAZYs) as well as other proteins were upregulated in lignin medium. 47 CAZYs genes of glycoside hydrolase, carbohydrate esterase (CE) or polysaccharide lyase (PL) families had significantly different transcript abundance in LIG3d relative to GLU3d (Additional file 2). The GHs mainly consisted of cellulose-degrading enzymes (GH6), hemicellulose-degrading enzymes (GH10/GH43/GH51), and pectin-degrading enzymes (GH28/GH78/GH88). These enzymes might be to hydrolyze a small amount of carbohydrate remained in lignin, and required for fungal growth. In particular, genes related to CAZYs including trehalase, chitinase, and mannosidase were upregulated. These enzymes might liberate carbon from major storage compound trehalose and be involved in fungal hyphal cell wall biosynthesis for growth [21, 31].

Numerous genes involved in mobilizing and recycling nitrogen were also expressed, including oligopeptide transporter, nucleoside transporter, acetamidase, amino acid permease, amine oxidase, arginase, aspartokinase, methionine synthase, nitrilase, and proteases (Additional file 3). In accordance with the abundance in the extracellular culture filtrates, polyporopepsins, and aspartic protease genes were early induced by lignin (LIG3d). Notably, polyporopepsin gene 0925.239 had the most expression level among extracellular proteases. In addition, acetamidases and amino acid permease genes were
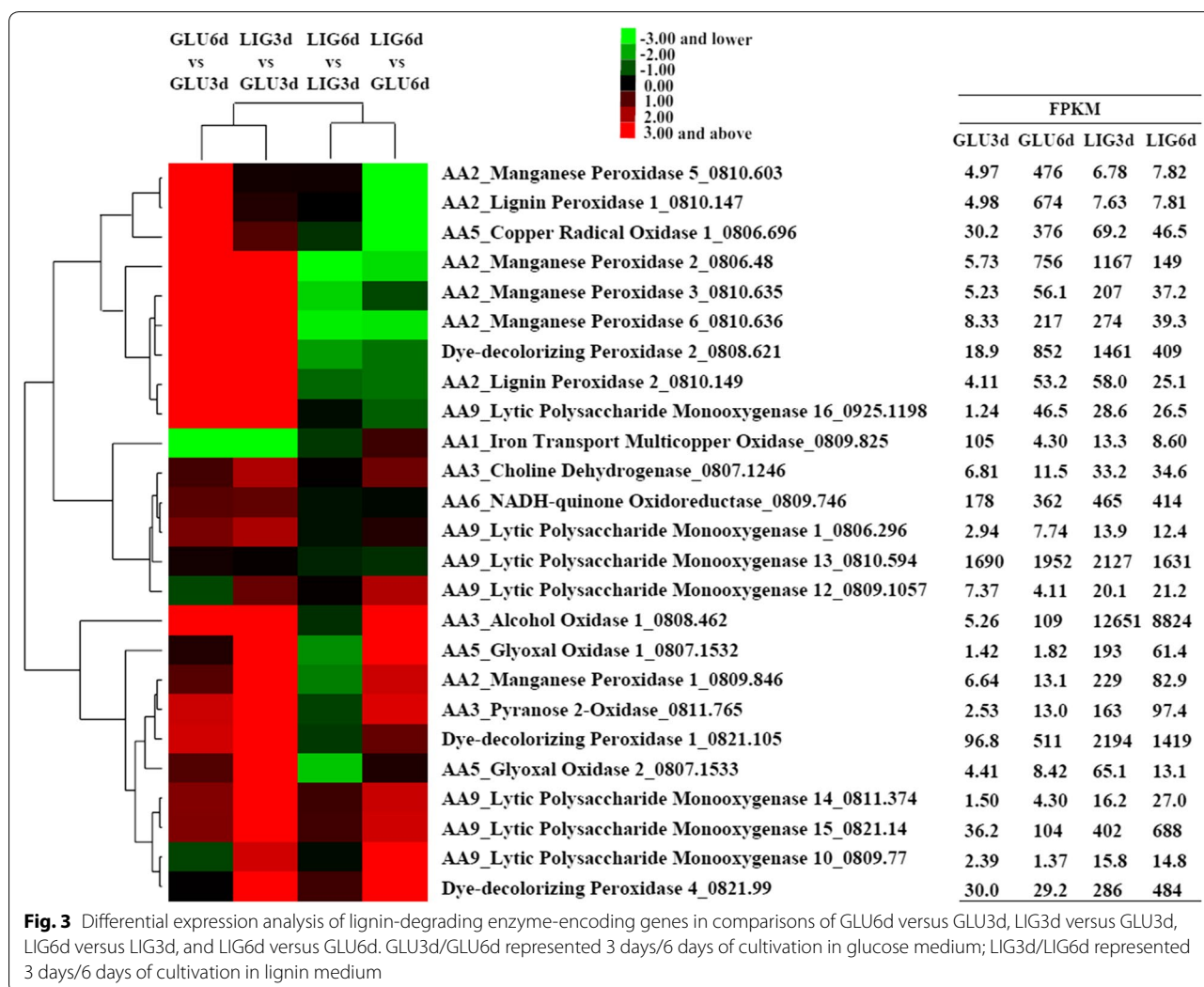
Qin *et al. Biotechnol Biofuels* (2018) 11:302

Page 5 of 11

Fig. 3 Differential expression analysis of lignin-degrading enzyme-encoding genes in comparisons of GLU6d versus GLU3d, LIG3d versus GLU3d, LIG6d versus LIG3d, and LIG6d versus GLU6d. GLU3d/GLU6d represented 3 days/6 days of cultivation in glucose medium; LIG3d/LIG6d represented 3 days/6 days of cultivation in lignin medium

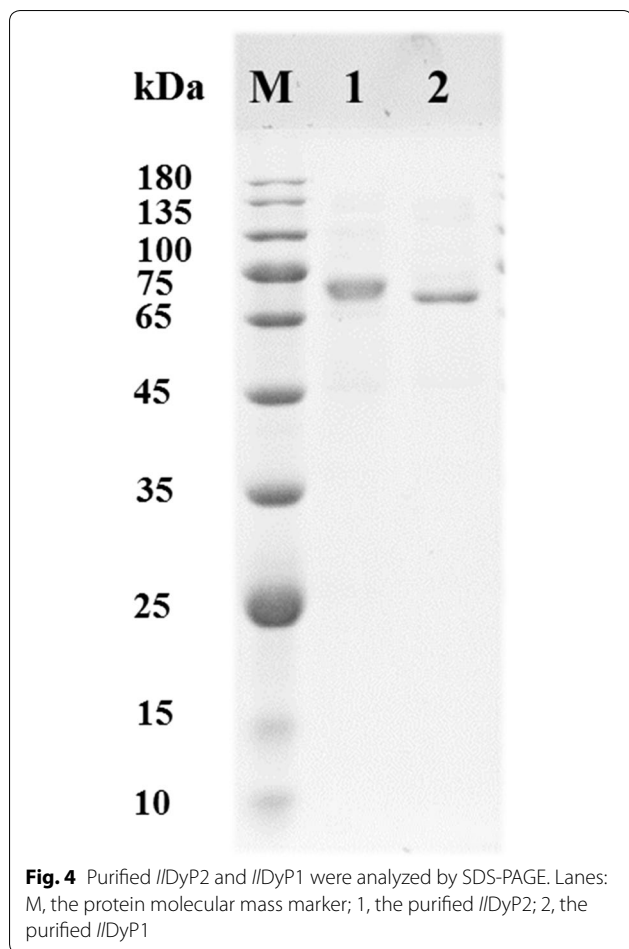significantly differentially accumulated in lignin medium (LIG3d and LIG6d).

The above results suggested that DyPs were the main extracellular ligninolytic enzymes of *I. lacteus* in lignin medium, while in lignocellulose medium MnPs played key roles [14]. Therefore, DyPs were purified from lignin medium for studying their characterization and catalytic properties.

Purification and characterization of DyPs from *I. lacteus* in lignin medium

Two DyP isoenzymes were purified to homogeneity from the liquid cultures of *I. lacteus* grown in alkali lignin medium for 3 days (Fig. 4). The molecular mass of *Il*DyP2 and *Il*DyP1 were about 74 kDa and 72 kDa, respectively. Like other classic heme peroxidases (e.g., MnP, VP, and LiP), DyPs also contain heme group judging from the absorbance at 410 nm [5, 16, 32]. The Rz (A_{410}/A_{280}) ratios of purified DyPs were 2.5 and 1.0, respectively.

Meanwhile, in order to identify corresponding DyP isoenzymes expressed in *I. lacteus* CD2, purified DyPs were separated from SDS-PAGE to digested for peptide mass fingerprinting analysis. Based on the number of unique peptides matched in DyPs from *I. lacteus*, *Il*DyP2 and *Il*DyP1 corresponded to genes 0808.621 and 0821.105, respectively (Table 2).

The optimal pH for *Il*DyP2 and *Il*DyP1 was determined in pHs ranging from 2 to 7 among six different substrates, including high redox potential dyes (RB19 and RB5), lignin model compounds (DMP, guaiacol, and VA) and ABTS (Fig. 5). *Il*DyP2 and *Il*DyP1 showed the same optimal pH 4.0 for oxidation of RB19 and guaiacol, in agreement with DyP for RB19 from *I. lacteus* CCBAS 238 [16]. *Il*DyP2 showed acidic optima for guaiacol (67%, 95%, and 57% of residual activities at pH 2, pH3, and pH 5, respectively), while *Il*DyP1 was found to show less acidic optima (9%, 52%, and 90% of residual activities at pH 2, pH3, and pH 5, respectively). However, only *Il*DyP2 could oxidize

Qin *et al. Biotechnol Biofuels*   (2018) 11:302

Page 6 of 11

Fig. 4 Purified *Il*DyP2 and *Il*DyP1 were analyzed by SDS-PAGE. Lanes: M, the protein molecular mass marker; 1, the purified *Il*DyP2; 2, the purified *Il*DyP1

RB5 in the narrow pH range from 3.0 to 4.0, which was slightly different from DyP in *I. lacteus* CCBAS 238 with optimal pH 3 and retaining 60% of residual activity at pH 2 for RB5. The optimal pH of 3.0 and 4.0 for *Il*DyP2 and *Il*DyP1 against VA and ABTS, respectively, and pH 4 for *Il*DyP1 could retain 80% of residual activity against VA and ABTS, while DyP in *I. lacteus* CCBAS 238 had optimal pH 2 for VA and pH 3 for ABTS, and retained 10% and 60% of residual activities at pH 4 for VA and ABTS, respectively. *Il*DyP2 and *Il*DyP1 showed the same optimal pH 3.0 for DMP, in accordance with DyP in *I. lacteus* CCBAS 238 [16]. *Il*DyP2 showed acidic optima of DMP (74%, 81%, and 55% of residual activity at pH 2, pH4, and pH 5, respectively), while *Il*DyP1 was found to show less acidic optima (14%, 98% and 76% of residual activity at pH 2, pH 4, and pH 5, respectively). The optimal values of DyPs in this study were very near to those of DyP from *Auricularia auricula-judae* (pH 3.5 for RB19, pH 2.5 for VA, and pH 3.0 for DMP, ABTS, and RB5) [33]. Liers et al. [7] observed that all DyPs tested showed rather acidic pH optima (pH 1.4–2.5) for oxidizing non-phenolic aromatics.

These differences in biochemical properties of DyP isoenzymes might be attributed to their divergent evolutionary origin. Furthermore, DyP isoenzymes had complementary effects on different pH values, the combination of *Il*DyP2 and *Il*DyP1 isoenzymes might result in wider pH range for efficient lignin degradation.

The catalytic properties of *Il*DyP2 and *Il*DyP1 for classic fungal heme peroxidases substrates ABTS, DMP, and guaiacol were presented in Table 3. *Il*DyP2 and *Il*DyP1

Table 2 Matching peptides with DyPs from *I. lacteus* after *Il*DyP2 and *Il*DyP1 trypsin digestion and PMF analysis

Protein accession	Peptide	Unique	Mass	*m/z*	Start	End
*Il*DyP2_0808.621	R.TNDPVTNRPSWALDGSFLVFR.K	Y	2391.2	798.07	254	274
	K.SEPLGLDPVIGQGTR.Q	Y	1537.81	513.61	443	457
	R.GLAFVEYQSVISNGFR.F	Y	1785.9	893.96	411	426
	R.NNDFNYIHPGEDLTTDETR.C	Y	2249.98	1126	340	358
	K.LKQLVPEFHK.W	Y	1237.72	619.87	276	285
	K.QLVPEFHK.W	Y	996.54	499.28	278	285
	R.C(+ 57.02)*PFTAHVR.K	Y	986.48	494.25	359	366
	R.QTFGLDPR.N	Y	932.47	467.24	458	465
	R.KLKQLVPEFHK.W	Y	1365.81	456.28	275	285
	K.GTNVDGVFLIGSDDVTTTNQYRDDLK.A	Y	2842.36	948.46	167	192
	R.WNSGAPIDLTPDVDDPTLGNDPQR.N	Y	2592.21	1297.11	316	339
*Il*DyP1_0821.105	R.TQQEVWANAAAFPFGK.T	Y	1763.86	882.94	424	439
	R.AGTPYGPELTDDESSSGTTSTDR.G	Y	2343	1172.51	385	407
	K.SGAPIDLSPDVDDASLGTDPQR.N	Y	2225.04	1113.53	317	338
	K.TESIGLDPVIGQGDR.T	Y	1555.78	778.9	440	454
	R.DLESVIGHANHAIR.A	Y	1530.79	766.4	371	384
	K.QLVPEFNK.W	Y	973.52	487.77	277	284

Qin *et al. Biotechnol Biofuels*   (2018) 11:302

Page 7 of 11

Fig. 5 Optimum pH of the purified IlDyP2 and IlDyP1 oxidizing different substrates: ABTS (**a**); lignin model compounds DMP (**b**), guaiacol (**c**) and VA (**d**); high redox potential dyes RB19 (**e**) and RB5 (**f**)
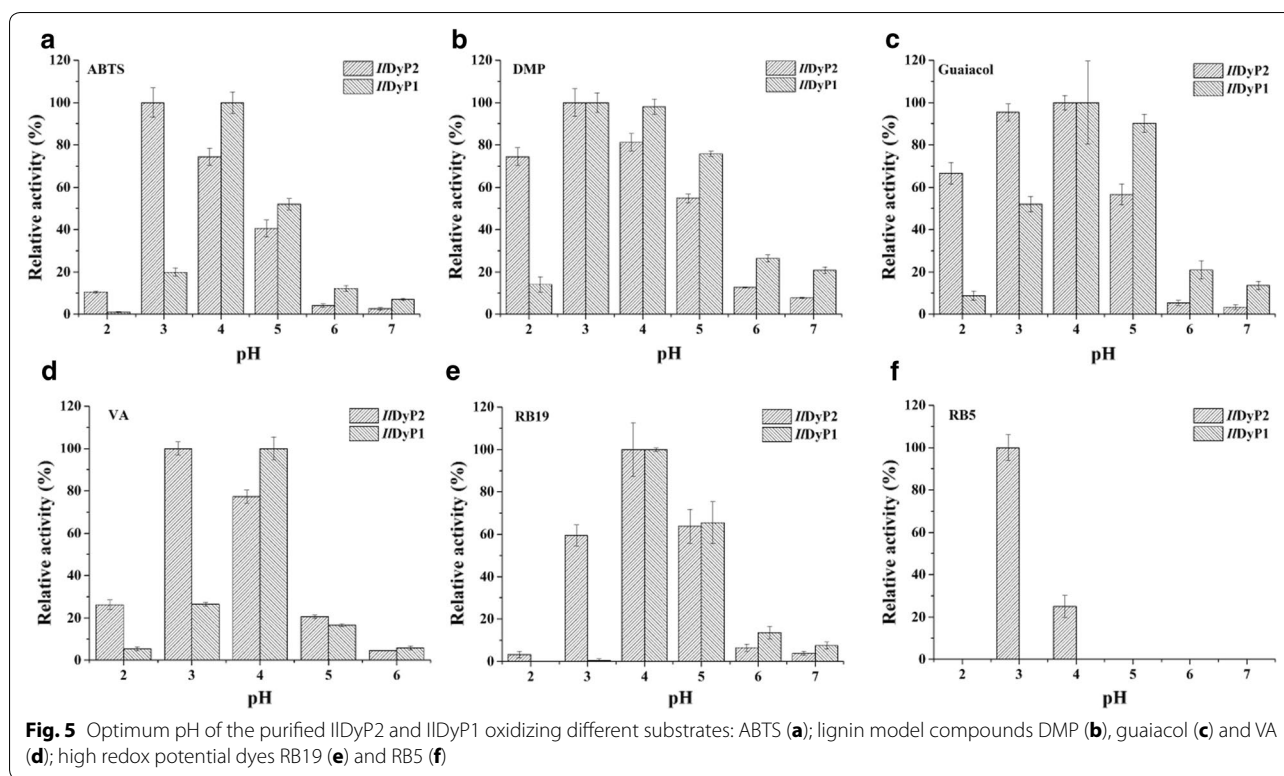
Table 3 Kinetic constants for oxidation of ABTS, DMP, and guaiacol by *Il*DyP2 and *Il*DyP1 from *I. lacteus*

Substrate	pH	*Il*DyP	K_m [μM]	k_{cat} [s^{-1}]	k_{cat}/K_m [s^{-1} M^{-1}]
ABTS	3	II	125.0 ± 1.4	396.2 ± 0.0	$(3.2 \pm 0.0) \times 10^6$
	4	I	693.1 ± 8.5	356.3 ± 11.2	$(5.1 \pm 0.1) \times 10^5$
DMP	3	II	1631.7 ± 10.9	560.8 ± 19.3	$(3.4 \pm 0.2) \times 10^5$
	4	I	892.7 ± 81.5	198.8 ± 12.6	$(2.2 \pm 0.1) \times 10^5$
Guaiacol	3	II	229.1 ± 15.9	49.7 ± 0.9	$(2.2 \pm 0.1) \times 10^5$
	4	I	592.1 ± 53.0	49.2 ± 1.5	$(8.3 \pm 0.5) \times 10^4$

exhibited significant differences in catalytic efficiencies for different substrates. K_m of *Il*DyP1 toward three substrates was higher than that of *Il*DyP2, suggesting that *Il*DyP2 had higher affinity for three substrates. *Il*DyP2 and *Il*DyP1 had similar activity for ABTS and guaiacol, while *Il*DyP2 had higher activity for DMP than for *Il*DyP1. *Il*DyP2 had sixfold and threefold higher catalytic efficiencies than *Il*DyP1 for ABTS and guaiacol. This suggested that *Il*DyP2 had better substrate fitting at the oxidation site, which was in accordance with the lack of activity of *Il*DyP1 on the recalcitrant dye RB5 [10]. In comparison with other typical fungal heme peroxidases, *Il*DyP2 and *Il*DyP1 displayed higher catalytic efficiencies for the oxidation of ABTS and DMP [34, 35].

In addition, the data shown in Fig. 5 revealed that the substrate specificities of *Il*DyP2 and *Il*DyP1 were similar to that of classic fungal heme peroxidases. *Il*DyP2 and *Il*DyP1 were both able to decolorize the high redox potential anthraquinone dye RB19, which is the common feature of all DyP-type peroxidases [8]. Notably, *Il*DyP2 had the ability to decolorize the recalcitrant dye RB5, while *Il*DyP1 could not decolorize RB5. Although *Il*DyP2 and *Il*DyP1 could not oxidize Mn^{2+} to Mn^{3+}, they could catalyze the oxidation of typical peroxidases substrates ABTS as well as phenolic lignin compounds DMP and guaiacol. Moreover, they exhibited low activity to oxidize non-phenolic lignin compound VA through peroxidase activity, belonging to the classic high redox potential peroxidases LiP and VP [2, 36]. It was also reported that other fungal DyPs can oxidize VA with very low activities [7, 35]. DyP in *I. lacteus* CCBAS 238 showed low activities for VA and RB5 [16]. In this study, we observed that mediator 1-HBT could promote VA degradation by *Il*DyP1. This phenomenon is similar to the oxidation of a non-phenolic lignin model compound by the laccase/1-HBT redox system [6, 37]. With 1-HBT as mediator, the oxidation rate of VA to veratraldehyde increased by 29.4% (Fig. 6). Considering their catalytic versatility, *Il*DyP2 and *Il*DyP1 might be a part of the alternative biocatalytic system for lignin degradation by *I. lacteus*, combining the catalytic properties of heme peroxidases and laccase.
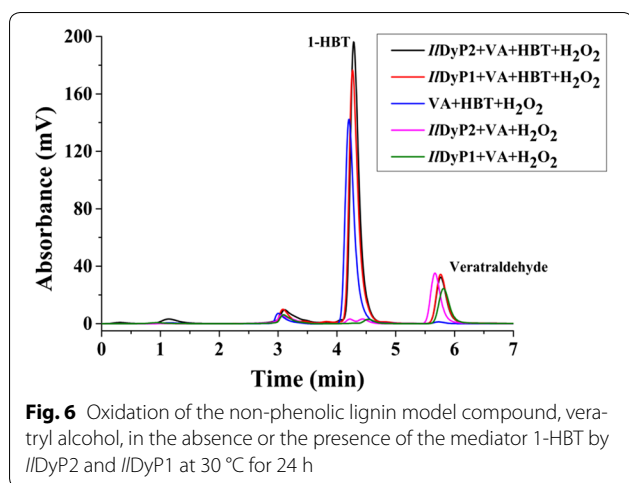
Qin *et al. Biotechnol Biofuels* (2018) 11:302

Page 8 of 11

Fig. 6 Oxidation of the non-phenolic lignin model compound, veratryl alcohol, in the absence or the presence of the mediator 1-HBT by *Il*DyP2 and *Il*DyP1 at 30 °C for 24 h

Some proteins in DyP family have low amino acid sequence identity (lower than 15%), and significant differences in catalytic efficiency (k_{cat}/K_m) with a few orders of magnitude [38]. Bacterial DyPs possess a lower oxidizing ability than fungal DyPs, oxidizing only less recalcitrant phenolic lignin model compounds and monophenolic substrates [39]. However, Chen et al. found DyP from *Thermomonospora curvata* showed high catalytic efficiency with ABTS, close to that of fungal DyPs [40]. Except for dye decolorization, DyP from *Raoultella ornithinolytica* OKOH-1 can directly decolorize melanin, and immobilization can improve its activity and stability [41]. Whereas only a limited number of DyPs were purified and characterized. Further studies are still needed to assess the precise physiological roles and catalytic properties of DyPs, including fungal DyPs.

Conclusions

Irpex lacteus CD2 grown in lignin medium secreted DyPs as the main extracellular ligninolytic enzymes. Transcriptomics analysis revealed that DyPs- and H_2O_2-generating enzymes including AOX, POX, and GLOX were coordinately expressed for efficient lignin degradation. Moreover, *Il*DyP2 and *Il*DyP1 could catalyze the oxidation of typical peroxidases substrates ABTS, phenolic lignin compounds DMP, and guaiacol as well as non-phenolic lignin compound VA. *Il*DyP1 could enhance the oxidation of non-phenolic lignin compound VA in the presence of mediator 1-HBT, the same as with Lac. These results proved for the first time that DyPs might depolymerize lignin when lacking classic heme peroxidases such as MnP, LiP, and Lac. DyPs could display different catalytic features of different peroxidases to different substrates, combining the catalytic properties of classic heme peroxidases and Lac. Therefore, DyPs may form an

important constituent of the ligninolytic system in wood-decaying fungi.

Materials and methods
Chemicals
Alkali lignin, 2,2′-azino-bis (3-ethylbenzothiazoline-6-sulfonic acid) (ABTS), 2,6-dimethylphenol (DMP), guaiacol, reactive black 5 (RB5), veratryl alcohol (VA), and 1-hydroxybenzotriazole (1-HBT) were purchased from Sigma-Aldrich (St. Louis, MO). Reactive blue 19 (RB19) was purchased from Sinopharm Chemical Reagent Company (Beijing, China).

Strain and culture conditions
Irpex lacteus CD2 [14] was maintained at 4 °C on potato dextrose agar plate. The inoculum was precultured in potato dextrose broth for 7 days at 28 °C, then 10% (v/v) inoculum was transferred into the modified Kirk's medium, and shaken at 150 rpm. The Kirk's medium contained: alkali lignin (or glucose) as the sole carbon source, 10 g/L; ammonium tartrate, 0.2 g/L; KH_2PO_4, 2 g/L; $MgSO_4 \cdot 7H_2O$, 0.71 g/L; $CaCl_2$, 0.1 g/L; and 70 mL trace element solution. The trace element solution contains NaCl, 1 g/L; $CoCl_2 \cdot 6H_2O$, 0.184 g/L; $FeSO_4 \cdot 7H_2O$, 0.1 g/L; $ZnSO_4 \cdot 7H_2O$, 0.1 g/L; $CuSO_4$, 0.1 g/L; H_3BO_3, 0.01 g/L; $Na_2MoO_4 \cdot 2H_2O$, 0.01 g/L; $KAl(SO_4)_2 \cdot 12H_2O$, 0.01 g/L; and nitrilotriacetic acid, 1.5 g/L.

Enzymatic assays
Total ligninolytic enzyme activities were measured by monitoring the oxidation of ABTS ($\varepsilon_{420} = 36{,}000$ M^{-1} cm^{-1}) at 420 nm, in 50 mM sodium tartrate buffer (pH 4.0) containing 1 mM ABTS, 1 mM Mn^{2+}, and 0.1 mM H_2O_2. Manganese-independent peroxidase activity was also determined by ABTS oxidation in the absence of Mn^{2+}. DyP activity was assayed by the decolorization of an anthraquinone dye RB19 ($\varepsilon_{595} = 10{,}000$ M^{-1} cm^{-1}) at 595 nm. The reaction was performed in the same buffer containing 125 μM RB19 and 0.1 mM H_2O_2. One unit of enzyme activity was defined as the amount of enzyme that oxidized 1 μmol of ABTS or RB19 per minute at 25 °C.

Secretome analysis
The extracellular enzymes of *I. lacteus* CD2 grown in alkali lignin at different periods of time were collected and concentrated by 80% ammonium sulfate [14]. The concentrated proteins were separated by one-dimensional SDS-PAGE, and the main bands on the third day were excised from the gel, digested with trypsin, and identified by nano LC–MS/MS. The peptides were separated in a reverse-phase C18 column, 0.18 mm × 100 mm, 5 μm particle size (Thermo). The mobile phases were A

Qin *et al. Biotechnol Biofuels*   (2018) 11:302

Page 9 of 11

(water) and B (acetonitrile) containing 0.1% formic acid [22]. The flow rate was maintained at 300 nL/min. The phase B gradient was started at 3%, followed by a linear gradient to 8% in 1 min, 8–40% in 5 min, 40–85% in 1 min, and held there for 1 min. All MS/MS spectra were searched using PEAKS software against *I. lacteus* CD2 protein database using the following criteria [42]: enzyme trypsin; fixed modification of cysteine ($+$57.02 Da); and variable modification of methionine ($+$15.99 Da).

Transcriptome analysis

Irpex lacteus CD2 was grown in the modified Kirk's medium containing lignin or glucose as carbon source. The total RNA was extracted from mycelia on days 3 and 6 using the TRIZOL reagent (Invitrogen, Waltham, MA) according to the manufacturer's instructions. The total RNA was sent to Annoroad Genomics (Beijing, China) for sample preparation and sequencing. All samples were in duplicate. The cDNA was synthesized and prepared for sequencing using the Illumina mRNA-Seq Sample Prep Kit (San Diego, CA). The samples were run on independent lanes, and paired-end sequences of 150 bp were obtained at 4 Gb clean data for each sample using the Illumina Hiseq 2500. The raw reads were trimmed and filtered using Trimmomatic software to remove adapters and low-quality bases [43]. Then clean reads were assembled into transcripts using TopHat and Cufflinks with the *I. lacteus* CD2 genome as a Ref. [14, 44]. All sequences of transcripts were extracted from reference sequence using gffread from cufflinks pipeline. The gene expression levels were conducted using the fragments per kilobase of exon per million fragments (FPKM) mapped method [45], and read counts were analyzed for differential expression using DESeq with a *q* value < 0.05 [46].

Purification and characterization of *Il*DyPs

The liquid cultures of *I. lacteus* CD2 grown in alkali lignin for 3 days were collected and concentrated by 80% ammonium sulfate at 4 °C. 20 mM sodium acetate buffer (pH 5.0) was used to dissolve the pellets and dialyzed using 30-kDa cutoff membrane. Then *Il*DyPs were purified using a HiTrap Q HP anion exchange column (GE Health, Fairfield, CT) pre-equilibrated with the same acetate buffer. The *Il*DyPs were eluted with a linear gradient of 0–1.0 M NaCl, and fractions containing active enzymes were pooled after SDS-PAGE. Meanwhile, the bands were excised and identified by peptide mass fingerprinting.

To determine the optimal pH, 50 mM sodium tartrate buffers with pH ranging from 2.0 to 7.0 were used for all substrates including ABTS, DMP, guaiacol, VA, RB19, and RB5 at 25 °C. The maximum activities of *Il*DyP2 and *Il*DyP1 were considered to be 100%. For catalysis

properties, the reactions were performed in optimal pH at 25 °C using 50–4000 μM substrates by monitoring corresponding oxidation products. The nonlinear least square fitting method was used to calculate the K_m, k_{cat}, and k_{cat}/K_m parameters of *Il*DyP2 and *Il*DyP1 using the GraphPad Prism 5 software.

1-HBT was used as the mediator in evaluating the abilities of *Il*DyP1 and *Il*DyP2 to oxidize the non-phenolic lignin compound VA. The oxidation of VA was performed in 50 mM sodium tartrate buffer (pH 4.0 or pH 3.0) containing 1 mM VA, 1 mM 1-HBT, 0.1 mM H_2O_2, and 0.5 U/mL *Il*DyP1 or *Il*DyP2, without 1-HBT or DyP as corresponding control. The reaction proceeded at 30 °C. After 24 h, the reaction products were analyzed by HPLC using a reverse-phase C18 column, 4.6 mm × 250 mm, 5-m particle size (Waters XTerra). The isocratic elution condition was performed with 55% methanol containing 0.1% formic acid at a flow rate of 1 mL/min. The elution peaks were monitored at 310 nm.

Additional files

Additional file 1. Proteins identification from *I. lacteus* secretome in kirk's medium supplemented with lignin on the third day.

Additional file 2. Transcript levels of *I. lacteus* genes encoding carbohydrate active enzymes in GLU3d, GLU6d, LIG3d and LIG6d.

Additional file 3. Transcript levels of *I. lacteus* genes involved in mobilizing and recycling nitrogen in GLU3d, GLU6d, LIG3d and LIG6d.

Qin *et al. Biotechnol Biofuels*   (2018) 11:302

Page 10 of 11

References

1. Azadi P, Inderwildi OR, Farnood R, King DA. Liquid fuels, hydrogen and chemicals from lignin: a critical review. Renew Sustain Energy Rev. 2013;21:506–23.
2. Camarero S, Sarkar S, Ruiz-Duenas FJ, Martinez MJ, Martinez AT. Description of a versatile peroxidase involved in the natural degradation of lignin that has both manganese peroxidase and lignin peroxidase substrate interaction sites. J Biol Chem. 1999;274:10324–30.
3. Ruiz-Duenas FJ, Martinez AT. Microbial degradation of lignin: how a bulky recalcitrant polymer is efficiently recycled in nature and how we can take advantage of this. Microb Biotechnol. 2009;2:164–77.
4. Kersten P, Cullen D. Extracellular oxidative systems of the lignin-degrading basidiomycete *Phanerochaete chrysosporium*. Fungal Genet Biol. 2007;44:77–87.
5. Janusz G, Kucharzyk KH, Pawlik A, Staszczak M, Paszczynski AJ. Fungal laccase, manganese peroxidase and lignin peroxidase: gene expression and regulation. Enzyme Microb Technol. 2013;52:1–12.
6. Cañas AI, Camarero S. Laccases and their natural mediators: biotechnological tools for sustainable eco-friendly processes. Biotechnol Adv. 2010;28:694–705.
7. Liers C, Pecyna MJ, Kellner H, Worrich A, Zorn H, Steffen KT, Hofrichter M, Ullrich R. Substrate oxidation by dye-decolorizing peroxidases (DyPs) from wood- and litter-degrading agaricomycetes compared to other fungal and plant heme-peroxidases. Appl Microbiol Biotechnol. 2013;97:5839–49.
8. Hofrichter M, Ullrich R, Pecyna MJ, Liers C, Lundell T. New and classic families of secreted fungal heme peroxidases. Appl Microbiol Biotechnol. 2010;87:871–97.
9. Sugano Y, Muramatsu R, Ichiyanagi A, Sato T, Shoda M. DyP, a unique dye-decolorizing peroxidase, represents a novel heme peroxidase family: ASP171 replaces the distal histidine of classical peroxidases. J Biol Chem. 2007;282:36652–8.
10. Fernandez-Fueyo E, Linde D, Almendral D, Lopez-Lucendo MF, Ruiz-Duenas FJ, Martinez AT. Description of the first fungal dye-decolorizing peroxidase oxidizing manganese (II). Appl Microbiol Biotechnol. 2015;99:8927–42.
11. Liers C, Bobeth C, Pecyna M, Ullrich R, Hofrichter M. DyP-like peroxidases of the jelly fungus *Auricularia auricula-judae* oxidize non-phenolic lignin model compounds and high-redox potential dyes. Appl Microbiol Biotechnol. 2010;85:1869–79.
12. Novotný Č, Cajthaml T, Svobodová K, Šušla M, Šašek V. *Irpex lacteus*, a white-rot fungus with biotechnological potential—review. Folia Microbiol. 2009;54:375–90.
13. Xu C, Ma F, Zhang X, Chen S. Biological pretreatment of corn stover by *Irpex lacteus* for enzymatic hydrolysis. J Agric Food Chem. 2010;58:10893–8.
14. Qin X, Su X, Luo H, Ma R, Yao B, Ma F. Deciphering lignocellulose deconstruction by the white rot fungus *Irpex lacteus* based on genomic and transcriptomic analyses. Biotechnol Biofuels. 2018;11:58.
15. Qin X, Sun X, Huang H, Bai Y, Wang Y, Luo H, Yao B, Zhang X, Su X. Oxidation of a non-phenolic lignin model compound by two *Irpex lacteus* manganese peroxidases: evidence for implication of carboxylate and radicals. Biotechnol Biofuels. 2017;10:103.
16. Salvachúa D, Prieto A, Martínez ÁT, Martínez MJ. Characterization of a novel dye-decolorizing peroxidase (DyP)-type enzyme from *Irpex lacteus* and its application in enzymatic hydrolysis of wheat straw. Appl Environ Microbiol. 2013;79:4316–24.
17. Svobodová K, Majcherczyk A, Novotný Č, Kües U. Implication of mycelium-associated laccase from *Irpex lacteus* in the decolorization of synthetic dyes. Bioresour Technol. 2008;99:463–71.
18. Qin X, Zhang J, Zhang X, Yang Y. Induction, purification and characterization of a novel manganese peroxidase from *Irpex lacteus* CD2 and its application in the decolorization of different types of dye. PLoS ONE. 2014;9:e113282.
19. Munoz C, Guillen F, Martinez AT, Martinez MJ. Induction and characterization of laccase in the ligninolytic fungus *Pleurotus eryngii*. Curr Microbiol. 1997;34:1–5.
20. Levasseur A, Drula E, Lombard V, Coutinho PM, Henrissat B. Expansion of the enzymatic repertoire of the CAZy database to integrate auxiliary redox enzymes. Biotechnol Biofuels. 2013;6:41.
21. Nitsche BM, Jørgensen TR, Akeroyd M, Meyer V, Ram AFJ. The carbon starvation response of *Aspergillus niger* during submerged cultivation: insights from the transcriptome and secretome. BMC Genomics. 2012;13:380.
22. Salvachúa D, Martínez AT, Tien M, López-Lucendo MF, García F, de los Ríos V, Martínez MJ, Prieto A. Differential proteomic analysis of the secretome of *Irpex lacteus* and other white-rot fungi during wheat straw pretreatment. Biotechnol Biofuels. 2013;6:115.
23. Sato S, Liu F, Koc H, Tien M. Expression analysis of extracellular proteins from *Phanerochaete chrysosporium* grown on different liquid and solid substrates. Microbiology. 2007;153:3023–33.
24. Li M, Liu X, Liu Z, Sun Y, Liu M, Wang X, Zhang H, Zheng X, Zhang Z. Glycoside hydrolase MoGls2 controls asexual/sexual development, cell wall integrity and infectious growth in the rice blast fungus. PLoS ONE. 2016;11:e0162243.
25. Carabajal M, Kellner H, Levin L, Jehmlich N, Hofrichter M, Ullrich R. The secretome of *Trametes versicolor* grown on tomato juice medium and purification of the secreted oxidoreductases including a versatile peroxidase. J Biotechnol. 2013;168:15–23.
26. Fernández-Fueyo E, Castanera R, Ruiz-Dueñas FJ, López-Lucendo MF, Ramírez L, Pisabarro AG, Martínez AT. Ligninolytic peroxidase gene expression by *Pleurotus ostreatus*: differential regulation in lignocellulose medium and effect of temperature and pH. Fungal Genet Biol. 2014;72:150–61.
27. Palmieri G, Giardina P, Bianco C, Fontanella B, Sannia G. Copper induction of laccase isoenzymes in the ligninolytic fungus *Pleurotus ostreatus*. Appl Environ Microbiol. 2000;66:920–4.
28. Daniel G, Volc J, Filonova L, Plíhal O, Kubátová E, Halada P. Characteristics of *Gloeophyllum trabeum* alcohol oxidase, an extracellular source of H_2O_2 in brown rot decay of wood. Appl Environ Microbiol. 2007;73:6241–53.
29. Daniel G, Volc J, Kubatova E. Pyranose oxidase, a major source of H_2O_2 during wood degradation by *Phanerochaete chrysosporium*, *Trametes versicolor*, and *Oudemansiella mucida*. Appl Environ Microbiol. 1994;60:2524–32.
30. Vanden Wymelenberg A, Gaskell J, Mozuch M, Kersten P, Sabat G, Martinez D, Cullen D. Transcriptome and secretome analyses of *Phanerochaete chrysosporium* reveal complex patterns of gene expression. Appl Environ Microbiol. 2009;75:4058–68.
31. Matsuzaki F, Shimizu M, Wariishi H. Proteomic and metabolomic analyses of the white-rot fungus *Phanerochaete chrysosporium* exposed to exogenous benzoic acid. J Proteome Res. 2008;7:2342–50.
32. Pérez-Boada M, Ruiz-Dueñas FJ, Pogni R, Basosi R, Choinowski T, Martínez MJ, Piontek K, Martínez AT. Versatile peroxidase oxidation of high redox potential aromatic compounds: site-directed mutagenesis, spectroscopic and crystallographic investigation of three long-range electron transfer pathways. J Mol Biol. 2005;354:385–402.
33. Linde D, et al. Catalytic surface radical in dye-decolorizing peroxidase: a computational, spectroscopic and site-directed mutagenesis study. Biochem J. 2015;466:253.
34. Fernandez-Fueyo E, Ruiz-Duenas FJ, Martinez MJ, Romero A, Hammel KE, Medrano FJ, Martinez AT. Ligninolytic peroxidase genes in the oyster mushroom genome: heterologous expression, molecular structure, catalytic and stability properties, and lignin-degrading ability. Biotechnol Biofuels. 2014;7:2.
35. Linde D, Coscolín C, Liers C, Hofrichter M, Martínez AT, Ruiz-Dueñas FJ. Heterologous expression and physicochemical characterization of a fungal dye-decolorizing peroxidase from *Auricularia auricula-judae*. Protein Expr Purif. 2014;103:28–37.
36. Sollewijn Gelpke MD, Lee J, Gold MH. Lignin peroxidase oxidation of veratryl alcohol: effects of the mutants H82A, Q222A, W171A, and F267L. Biochemistry. 2002;41:3498–506.

Qin *et al. Biotechnol Biofuels*   (2018) 11:302

Page 11 of 11

37. Bourbonnais R, Paice MG. Oxidation of non-phenolic substrates: an expanded role for laccase in lignin biodegradation. FEBS Lett. 1990;267:99–102.
38. Yoshida T, Sugano Y. A structural and functional perspective of DyP-type peroxidase family. Arch Biochem Biophysics. 2015;574:49–55.
39. de Gonzaloa G, Colpab DI, Habib MHM, Fraaije MW. Bacterial enzymes involved in lignin degradation. J Biotechnol. 2016;236:110–9.
40. Chen C, Shrestha R, Jia K, Gao PF, Geisbrecht BV, Bossmann SH, Shi J, Li P. Characterization of dye-decolorizing peroxidase (DyP) from *Thermomonospora curvata* reveals unique catalytic properties of A-type DyPs. J Biol Chem. 2015;290:23447–63.
41. Falade AO, Mabinya LV, Okoh AI, Nwodo UU. Biochemical and molecular characterization of a novel dye-decolourizing peroxidase from *Raoultella ornithinolytica* OKOH-1. Int J Biol Macromol. 2019;212:454–62.
42. Ma B, Zhang K, Hendrie C, Liang C, Li M, Doherty-Kirby A, Lajoie G. PEAKS: powerful software for peptide de novo sequencing by tandem mass spectrometry. Rapid Commun Mass Spectrom. 2003;17:2337–42.
43. Bolger AM, Lohse M, Usadel B. Trimmomatic: a flexible trimmer for Illumina sequence data. Bioinformatics. 2014;30:2114–20.
44. Trapnell C, Roberts A, Goff L, Pertea G, Kim D, Kelley DR, Pimentel H, Salzberg SL, Rinn JL, Pachter L. Differential gene and transcript expression analysis of RNA-seq experiments with TopHat and Cufflinks. Nat Protoc. 2012;7:562–78.
45. Trapnell C, Williams BA, Pertea G, Mortazavi A, Kwan G, van Baren MJ, Salzberg SL, Wold BJ, Pachter L. Transcript assembly and quantification by RNA-Seq reveals unannotated transcripts and isoform switching during cell differentiation. Nat Biotechnol. 2010;28:511.
46. Anders S, Huber W. Differential expression analysis for sequence count data. Genome Biol. 2010;11:R106.